

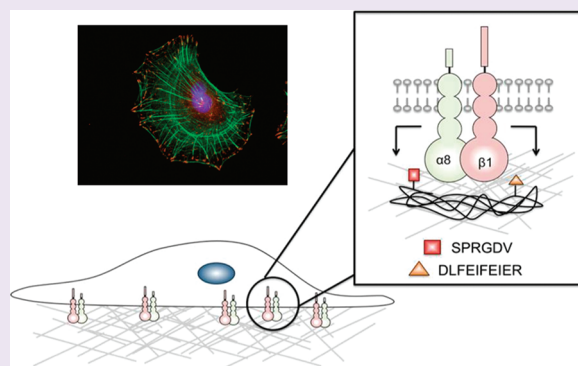
Using Self-Assembled Monolayers To Understand $\alpha 8\beta 1$ -Mediated Cell Adhesion to RGD and FEI Motifs in Nephronectin

Juan Sánchez-Cortés and Milan Mrksich*

Department of Chemistry and Howard Hughes Medical Institute, The University of Chicago, 929 East 57th Street, Chicago, Illinois 60637, United States

S Supporting Information

ABSTRACT: Nephronectin is an extracellular matrix protein that interacts with the $\alpha 8\beta 1$ integrin receptor and plays a role in tissue and organ development, though the motifs that mediate adhesion to the receptor remain unclear. This paper describes the use of self-assembled monolayers to study the adhesion of $\alpha 8\beta 1$ -presenting cells to the RGD and DLFEIFEIER ligands in nephronectin and found that both ligands can independently mediate cell adhesion through nonoverlapping binding sites on the integrin. Peptide truncation experiments showed FEI to be the minimal binding sequence within the DLFEIFEIER sequence, and adhesion experiments with peptides that include both the RGD and FEI sequences demonstrate that the two peptides bind synergistically to the receptor. Finally, a peptide array was used to establish a strict requirement for the glutamate residue of FEI and tolerance of other aromatic and hydrophobic residues in the first and third positions, respectively. This work provides an enhanced understanding of the binding of nephronectin with $\alpha 8\beta 1$ and identifies a peptide ligand that can be used for targeting the $\alpha 8\beta 1$ integrin.



Nephronectin is a novel extracellular matrix (ECM) protein that was first identified in studies of kidney development. Mice that lack this protein, or its integrin receptor $\alpha 8\beta 1$, display renal agenesis at birth. Previous work has implicated two sequences in nephronectin, RGD and DLFEIFEIER, that interact with the $\alpha 8\beta 1$ receptor, but characterization of the active ligands and their binding to the integrin remain incomplete. Here, we report the use of model substrates that present the nephronectin ligands against an otherwise inert background to study the role of each ligand in the absence of other specific or nonspecific interactions. We show that RGD and DLFEIFEIER bind the integrin to mediate adhesion when present individually and also interact synergistically with the integrin by binding to nonoverlapping sites (Figure 1). We also use a peptide array to identify the tripeptide FEI as the minimal binding motif and to define the consensus sequence for this ligand.

The discovery of nephronectin is closely related to the study of the integrin $\alpha 8\beta 1$ in neuronal pathways.¹ As $\alpha 8\beta 1$ interacts with extracellular matrix proteins, including fibronectin, vitronectin, and tenascin-c,² mice lacking the $\alpha 8$ subunit were generated to study the effects of this deletion in the nervous system. Surprisingly, mice lacking $\alpha 8$ failed to develop kidneys and pointed to an important role for this molecule in renal development. Using anti- $\alpha 8$ antibodies, it was found that this integrin subunit is expressed in the early stages of kidney development, with no detectable expression in later phases.³ Further, immunoprecipitation experiments found that the $\alpha 8$ subunit associates with the

$\beta 1$ subunit exclusively.³ Hence, this integrin was believed to play a causal role in aberrant kidney development.

The $\alpha 8\beta 1$ integrin binds to fibronectin, vitronectin and tenascin-c, yet none of these proteins are expressed in the appropriate spatiotemporal pattern to localize to the site of kidney development.³ Osteopontin, another known $\alpha 8\beta 1$ ligand, is deposited in the developing kidney, but mutation of its gene *in vivo* showed that it was not necessary for renal development.^{4,5} Using an $\alpha 8\beta 1$ -alkaline phosphatase (AP) soluble receptor, Reichardt and co-workers identified a novel gene product that bound to $\alpha 8\beta 1$ in mouse kidney extracts.⁶ The cDNA of this ligand was obtained using expression cloning screens and found to code for nephronectin, a secreted protein composed of five EGF-like domains joined to a MAM domain through a flexible linker. This linker contains an RGD triad, a canonical integrin-binding sequence, and competition experiments revealed that $\alpha 8\beta 1$ binds this RGD site. Nephronectin was also found to be expressed in mouse kidney tissue in a pattern that matched that of $\alpha 8\beta 1$, and mice lacking nephronectin showed similar phenotypes to mice lacking the $\alpha 8$ subunit.⁷ The protein was also found in other organs, suggesting that it has a wider role in tissue and organ development,⁶ including in preosteoblastic cells.⁸

Received: December 30, 2010

Accepted: July 26, 2011

Published: July 26, 2011

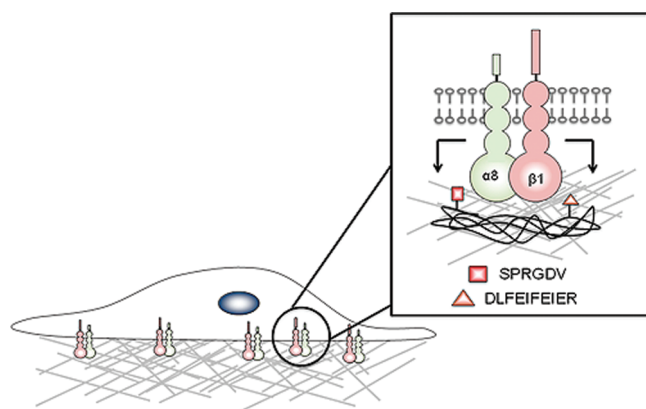


Figure 1. Integrin $\alpha 8\beta 1$ mediates cell adhesion to nephronectin, through interactions with the RGD and DLFEIFEIER peptide motifs.

Although nephronectin includes an RGD triad as part of its primary structure, early observations pointed to the presence of additional binding sites for cell-surface receptors. MC3T3-E1 cells, which express nephronectin endogenously, were able to adhere to recombinant nephronectin variants where the RGD sequence had been mutated to RGE, as were KA8 cells engineered to express $\alpha 8\beta 1$.⁸ Sekiguchi and co-workers found that the linker segment of nephronectin was active for binding to $\alpha 8\beta 1$.⁹ N-Terminal deletion mutants of this domain showed that the RGD motif was required for binding $\alpha 8\beta 1$, yet C-terminal deletion mutants where the RGD triad remained intact also showed a diminished ability to bind the receptor and suggested the presence of an additional ligand for $\alpha 8\beta 1$. Further deletions pointed to DLFEIFEIER, a sequence of nine residues downstream of RGD, and alanine scanning mutagenesis suggested EIE to be the minimal binding sequence in DLFEIFEIER. A peptide having both the RGD and EIE sequences could inhibit cell adhesion in a manner similar to that observed with wild-type nephronectin. When inhibition experiments were carried out with peptides that had either AIA in place of EIE or RGE in place of RGD, the peptides had to be present at concentrations that were 10-fold and 1000-fold higher, respectively, to achieve levels of inhibition that were comparable to those observed with the parent peptide. These results suggested that both ligands bind to the integrin and that the RGD has a higher affinity for the receptor than does EIE. Trans-complementation assays supported this interpretation and led to a model wherein $\alpha 8\beta 1$ has a bipartite binding site for the nephronectin motifs. These results were partially verified in cell adhesion assays, where HT1080 cells that expressed the $\alpha 8$ subunit adhered to recombinant proteins that had both RGD and EIE.⁹

The cell adhesion assays were carried out using culture substrates having an adsorbed layer of nephronectin variants. Although this method for preparing the substrates is simple, the immobilized protein has a heterogeneous activity, owing to varying orientations, conformations, and densities of protein, that make it difficult to control the fraction of adsorbed protein that presents ligand that is available for interacting with the cell surface receptor.¹⁰ It is also incorrect to assume that mutated proteins will adsorb in the same conformation as do the wild-type counterparts, even if the mutant differs at a single residue.¹¹ Finally, protein-coated substrates can be remodeled by cells, making it difficult to control the composition of adsorbed protein

during long-term experiments.¹² For those reasons, the present work used self-assembled monolayers as structurally well-defined mimics of the extracellular matrix in order to characterize the ligands from nephronectin that mediate $\alpha 8\beta 1$ -dependent cell adhesion.

RESULTS AND DISCUSSION

Model Substrates for $\alpha 8\beta 1$ -Mediated Cell Adhesion. We used model substrates that mimic the extracellular matrix to study the roles of SPRGD and DLFEIFEIER ligands in nephronectin. Because the latter peptide was insoluble, we added three Lys residues to the N-terminus. The peptides were all prepared in the N-acetylated form and were immobilized by applying solutions to a monolayer presenting maleimide groups at a density of 1% against a background of tri(ethylene glycol) groups (Figure 2A). SAMDI mass spectrometry was used to verify that each peptide had undergone efficient immobilization. For example, a mass spectrum of the monolayer presenting the SPRGDVC peptide showed the expected peaks for sodium adducts of the mixed disulfide containing one tri(ethylene glycol) group and one SPRGDVC peptide (m/z , 1666.3) as well as the SPRGDVC-terminated alkanethiolate (m/z , 1332.0) (Figure 2B). Similarly, the mass spectrum of the monolayer presenting the KKKDLFEIFEIERC peptide showed the expected peaks for sodium adducts of the mixed disulfide containing one tri(ethylene glycol) group and one KKKDLFEIFEIERC peptide (m/z , 2689.6) and the KKKDLFEIFEIERC-terminated alkanethiolate (m/z , 2355.4) (Figure 2C). The tri(ethylene glycol) groups are important because they prevent nonspecific protein adhesion and, therefore, remodeling of the matrix.¹⁰ Several studies have demonstrated the suitability of SAMs as model substrates for mechanistic studies of cell adhesion.^{13–16} We used H4 cells for all adhesion experiments in this work. This epithelial cell line expresses the $\alpha 8\beta 1$ integrin.¹⁷

Adhesion of H4 Cells to Monolayers Presenting SPRGDVC and KKKDLFEIFEIERC. We allowed H4 cells to adhere to monolayers presenting SPRGDVC, KKKDLFEIFEIERC, or SPRGDVFIPRQPTNDLFEIFEIERC at a density of 1% (relative to total alkanethiolate). All ligands mediated efficient adhesion of cells and spreading to give a flattened morphology (Figure 3A–C). Hence, for substrates presenting the ligands at this density, each ligand can efficiently mediate cell adhesion and spreading. As a positive control, we found that H4 cells adhered to a nephronectin-coated hydrophobic monolayer with a similar morphology (Figure 3D). Several control experiments establish that the observed adhesion was specific. First, cells failed to adhere to monolayers that present unreacted maleimide groups or to monolayers that present scrambled forms of the peptides (SPRDGC and KKKDLFEIFEIERC, data not shown). H4 cells also failed to adhere to monolayers presenting the peptide KKKC, suggesting that the addition of three Lys residues to the DLFEIFEIER peptide did not impart additional cell adhesion activity (data not shown). Finally, H4 cells failed to adhere to monolayers presenting only tri(ethylene glycol) groups (data not shown).

H4 Cells Adherent to SPRGDVC and KKKDLFEIFEIERC Had Well-Formed Cytoskeletons. We allowed cells to attach to monolayer substrates that presented SPRGDVC, KKKDLFEIFEIERC, or SPRGDVFIPRQPTNDLFEIFEIERC and then fixed the cultures to permit imaging of the cytoskeletal structures. We used an antipaxillin antibody to visualize focal adhesions and

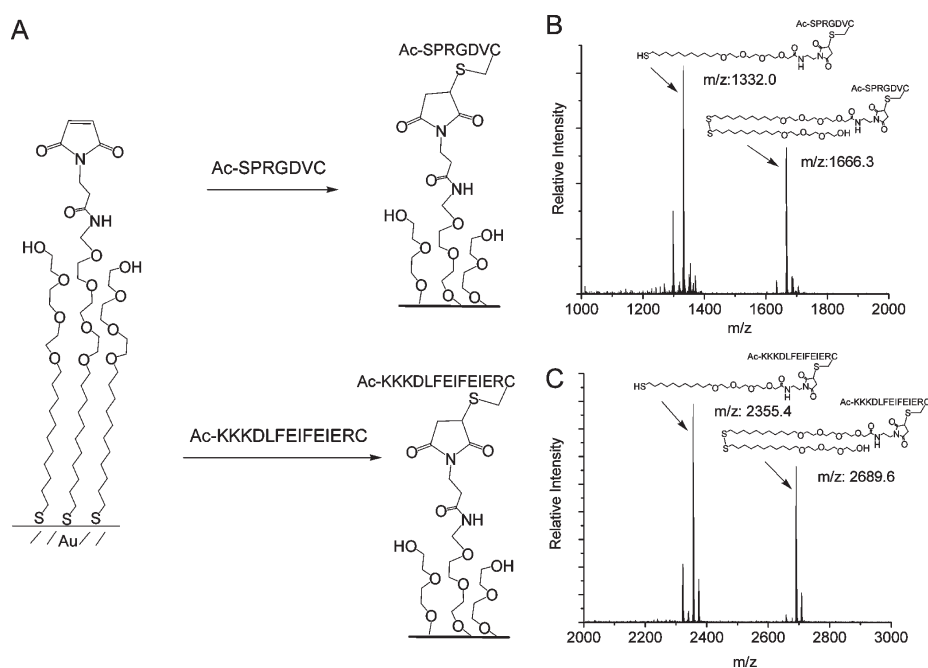


Figure 2. This work used self-assembled monolayers that present peptide ligands as model substrates for cell adhesion. A maleimide-terminated monolayer reacts with Cys-terminated peptides to afford surfaces that present the nephronectin ligands SPRGDVC and KKKDLFEIFEIERC (A). The tri(ethylene glycol) groups prevent nonspecific cell adhesion. The monolayers were characterized by SAMDI-MS with the peptides SPRGDVC (B) and KKKDLFEIFEIERC (C) present at a density of 1% relative to total alkanethiolate. The structures of the molecules detected in the SAMDI experiment are shown in the spectra and in each case were observed as the sodium ion adducts.

phalloidin AF 488 to visualize actin stress fibers. Nuclei were marked with DAPI. For monolayers presenting either SPRGDVC or KKKDLFEIFEIERC, the cells had well-developed focal adhesions distributed around the cell perimeter, with actin fibers that spanned the dimensions of the cell (Figure 3E and F). Cells adherent to the long peptide having both sequences also displayed similar cytoskeletal organization (Figure 3G). As a control, H4 cells adhered and showed similar cytoskeletal structure on substrates that were coated with recombinant nephronectin (Figure 3H). These results suggested that the nephronectin peptide ligands could mediate similar cytoskeletal phenotypes as does the full length protein.

A recent study by Sekiguchi and co-workers addressed the binding of nephronectin to the $\alpha 8\beta 1$ integrin. They compared cell adhesion to plates coated with nephronectin variants or GST-peptide fusions and also used soluble peptides to inhibit adhesion. That work found that a nephronectin variant having a mutated RGD motif was less efficient at supporting cell adhesion, but those studies did not examine cell adhesion to a nephronectin variant having the DLFEIFEIER sequence mutated.⁹ While this work is consistent with our finding that RGD and DLFEIFEIER interact with $\alpha 8\beta 1$, we observed that each ligand was capable of mediating adhesion alone. We suggest that the discrepancies arise from the use of protein-coated substrates as described above. The protein mutants could have adsorbed with different orientations or with different degrees of denaturation. In either event, our use of structurally well-defined substrates that present ligands with complete control of orientation and density avoids these limitations and leads to the unambiguous finding that both DLFEIFEIER and RGD can mediate comparable cell adhesion independently at this surface density.

Integrin Specificity for Ligands in Nephronectin. We used a panel of anti-integrin antibodies to determine which integrins

mediated adhesion to SPRGDVC and KKKDLFEIFEIERC (Figure 4). H4 cells were separately incubated with an anti- $\alpha 5$, anti- $\alpha 5$, or anti- $\beta 1$ antibody and then allowed to adhere to the monolayer substrates. The antibodies, alone or in combination, each decreased cell adhesion to SPRGDVC. This result is consistent with the known ability of the $\alpha 5\beta 1$ and $\alpha 8\beta 1$ integrins to bind the canonical RGD ligand. In contrast, we found that the anti- $\alpha 8$ and anti- $\beta 1$ antibodies, but not the anti- $\alpha 5$ antibody, decreased adhesion to monolayers presenting the KKKDLFEIFEIERC peptide. Taken together, these results suggest that both $\alpha 5\beta 1$ and $\alpha 8\beta 1$ can bind to nephronectin through its RGD sequence, but only $\alpha 8\beta 1$ can recognize nephronectin through its additional peptide ligand. This finding is consistent with several past reports that have shown that nephronectin is the specific ligand for integrin $\alpha 8\beta 1$ but also interacts with several other members of the integrin family.⁹

FEI Is the Minimal Binding Motif for $\alpha 8\beta 1$. We next compared the adhesion of H4 cells to peptide fragments derived from the DLFEIFEIER ligand in order to define the minimal binding sequence (Figure 5). Again, each of the truncated peptides was modified with three additional Lys residues at the N-terminus to impart solubility. A comparison of cell adhesion to KKKDLFEIC, KKKFEIERC, and KKKFEIFEIC, which correspond to the first five, last five, and middle six residues of the sequence, revealed that all three peptides supported cell adhesion and suggested that the FEI triad was the minimal binding sequence. Further studies with monolayers presenting N- and C-terminal truncations of the three peptides demonstrated that FEI was indeed the minimal binding sequence. These results show that the FEI motif is capable of supporting cell adhesion and also reveal that only one triad is necessary to engage $\alpha 8\beta 1$. Further experiments support this claim, as anti- $\alpha 8$ and anti- $\beta 1$, but not anti- $\alpha 5$ antibodies, inhibit H4 cell adhesion to the FEI

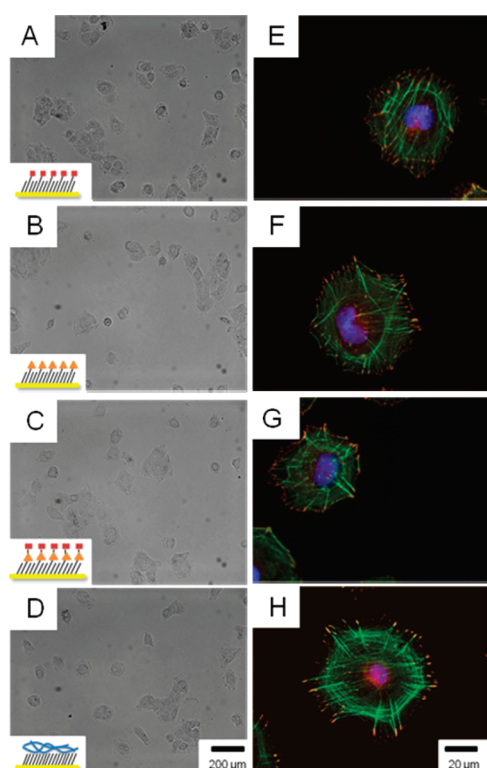


Figure 3. Adhesion and cytoskeletal structure of H4 cells on the model substrates. Optical micrographs of H4 cells that adhered and spread on monolayers presenting SPRGDVC ■ (A), KKKDLFEIFEIERC ▲ (B), and Ac-SPRGDVFIPRQPTCDLFEIFEIERC (C). As a positive control, H4 cells adhered to a methyl-terminated monolayer having an adsorbed layer of nephronectin (D). The scale bar in panel D applies to all phase contrast panels. Immunofluorescent staining of H4 cells on model substrates (E–H). Focal adhesions were visualized with an antipaxillin antibody (red), actin stress fibers were visualized with AF 488 phalloidin (green), and nuclei were visualized with DAPI (blue). The scale bar in panel H applies to all fluorescent panels.

peptide (Supplementary Figure 1A). Also, KA8 cells, engineered to display $\alpha 8\beta 1$, bound to monolayers presenting the FEI peptide, while the parent cell line lacking this integrin did not (Supplementary Figure 1B and C).

SPRGDV and KKKDLFEIFEIER Bind to Different Sites in $\alpha 8\beta 1$.

To elucidate whether each peptide interacts with the same or nonoverlapping sites in $\alpha 8\beta 1$, we determined whether either SPRGD or KKKDLFEIFEIER, in soluble form, could block the adhesion of cells to monolayers presenting the peptide ligands (Figure 6). We first verified that each peptide could block cell adhesion to a monolayer presenting the same ligand in a concentration-dependent manner. For example, SPRGD inhibited H4 cell adhesion to monolayers presenting SPRGDVC (Figure 6A), and KKKDLFEIFEIER inhibited attachment of cells to the monolayer presenting KKKDLFEIFEIERC (Figure 6B). This result demonstrates that adhesion to the monolayers was specific. We also found that each peptide was incapable of inhibiting cell adhesion to substrates presenting the other peptide. That is, soluble SPRGDV had no effect on H4 cell adhesion to a monolayer presenting the KKKDLFEIFEIERC peptide, and *vice versa*. This result suggests that the two peptide ligands bind to different sites in the integrin. Cell adhesion inhibition assays performed with soluble peptides having scrambled peptides, SPRDGV and KKKDLFEIFEIER,

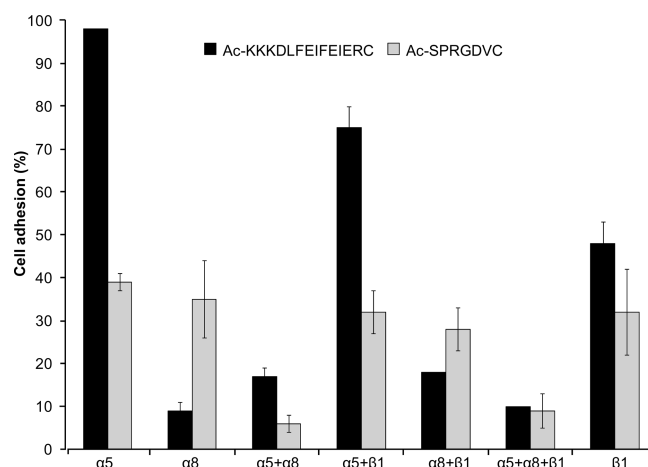


Figure 4. Effects of anti-integrin antibodies on H4 cell adhesion to model substrates. Cells were incubated with antibodies against $\alpha 5$, $\alpha 8$, and $\beta 1$, either individually or in combination, and then allowed to attach to monolayers presenting either the SPRGDVC peptide (light bars) or KKKDLFEIFEIERC peptide (black bars). Cell adhesion to monolayers presenting DLFEIFEIER peptide was partially inhibited by the $\alpha 8$ and $\beta 1$ antibodies. Cell adhesion to monolayers presenting SPRGDV peptide was partially inhibited by the $\alpha 5$, $\alpha 8$, and $\beta 1$ antibodies. Cell adhesion was quantitated as normalized units relative to adhesion in the absence of antibodies. Error bars are the standard error of three experiments.

were inactive in reducing cell adhesion, demonstrating the specificity of the ligand–receptor interactions discussed above. These experiments are consistent with the earlier report by Sato that found that $\alpha 8\beta 1$ binds to DLFEIFEIER and RGD through distinct binding sites.⁹ It is significant that our approach, which uses surfaces quite distinct from those used by Sato, led to a consistent conclusion since studies of cell adhesion can be complicated by artifacts associated with the substrate. Hence these two reports give a consistent understanding that the RGD and FEI motifs bind distinct sites on the receptor and will inform strategies to develop selective inhibitors for the $\alpha 8\beta 1$ receptor.

SPRGDV and KKKDLFEIFEIER Bind Synergistically to $\alpha 8\beta 1$.

To address whether the $\alpha 8\beta 1$ receptor binds the RGD and DLFEIFEIER ligands synergistically, that is, whether the affinity of the receptor for a peptide having both ligands is increased relative to that for either ligand alone, we compared the adhesion of H4 cells to monolayers presenting peptides at a range of densities. We compared the number of cells that attached per unit area as well as the degree of spreading for monolayers presenting Ac-SPRGDVC, Ac-KKKDLFEIFEIERC, and a long peptide, Ac-SPRGDVFIPRQPTNDLFEIFEIERC, containing both active sequences (Figure 7A and B). We found that the three peptides mediated comparable cell adhesion and spreading when present on monolayers at densities of 1% and 0.1%, yet the long peptide could support efficient adhesion and spreading when present at densities 100-fold lower than either of the short peptides alone. This finding points to a synergistic relationship between the ligands that leads to a higher affinity for binding the receptor. We found that monolayers presenting a mixture of the RGD and FEI ligands failed to give efficient cell adhesion at these densities, revealing that the arrangement of the ligands within the same peptide is important for the synergistic effect.

Structure–Activity Relationship of the FEI Peptide Triad.

We used a peptide array to determine the structural features of

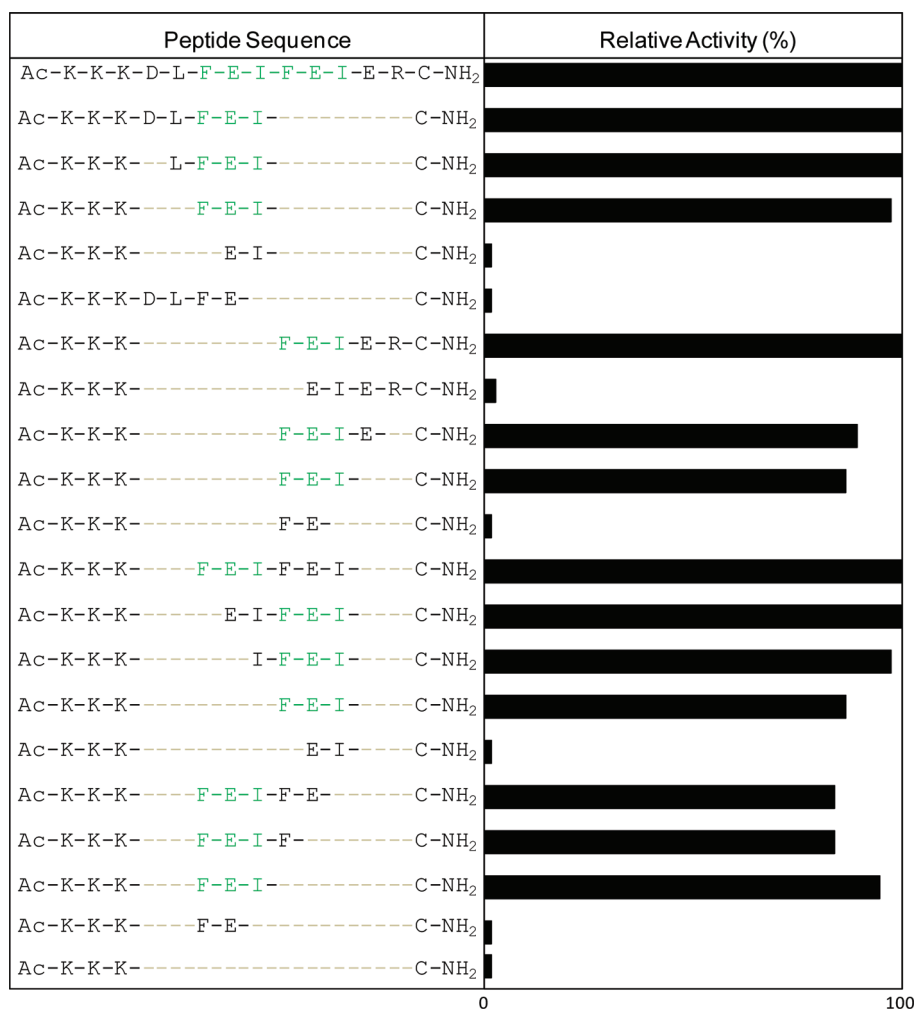


Figure 5. Cell adhesion experiments were performed using a series of monolayers presenting fragments of the DLFEIFEIER peptide. Only those peptides having the FEI motif (in green letters) were effective at mediating adhesion. The numbers of cells that adhered to each substrate are shown relative to adhesion on monolayers presenting the parent peptide, and are the average of three experiments. Error bars are omitted for clarity.

the FEI ligand that were important for receptor binding. We synthesized three sets of peptides where each of the three residues in FEI was individually replaced with an amino acid, that is, we prepared peptides of the form KKGXEIGC, KKGFXIGC, and KKGFEIXGC, where X represents each amino acid except cysteine. The 57 peptides were immobilized on an array of self-assembled monolayers and then used in cell adhesion experiments (Figure 8). For the “XEI” library, we found that the Phe residue could be replaced by Tyr or Trp and still support cell adhesion (Figure 8A). Interestingly, the “FXI” library showed a strict requirement for the Glu residue in the second position (Figure 8B). Finally, for the “FEX” library the Ile residue could be replaced by Ala, Leu, or Val and still support cell adhesion (Figure 8C). These results reveal a consensus sequence that requires an aromatic residue in the first position, a glutamate in the second position and a hydrophobic residue in the third position. We confirmed that cells adherent on monolayers presenting each of these ligands displayed cytoskeletal structures marked by paxillin-containing focal adhesions around the cell perimeter with actin fibers that spanned the cell area (Figure 8D–I). These results agree with a previous study that explored the sequence requirements for the ligand, including the importance of the glutamate residue, the loss of activity when

the phenylalanine residue was replaced with alanine, and the retention of activity when the isoleucine residue was replaced with alanine.⁹ Further, this example demonstrates the value of peptide arrays in both identifying adhesion ligands and in profiling the structural features of the ligands that are required for activity. We expect that this route will be important for identifying ligands for other receptors and for guiding the design of nonpeptide small molecules that antagonize receptor function.

Self-Assembled Monolayers As Models of the ECM. This work also demonstrates the characteristics of monolayers that make them well-suited for use as mimics of the ECM. Most importantly, the monolayers allow excellent control over the ligand–receptor interactions that mediate cell adhesion and that regulate signaling pathways in adherent cells. This benefit stems from the use of oligo(ethylene glycol) groups to reduce non-specific interactions and the ability to control the presentation of immobilized ligands, including the density, orientation, and even geometric pattern.¹⁰ Together, these characteristics address the limitations inherent in the use of protein-coated substrates and remove the ambiguities that complicate the interpretation of adhesion experiments on those substrates. The monolayers are also compatible with the standard protocols of cell culture

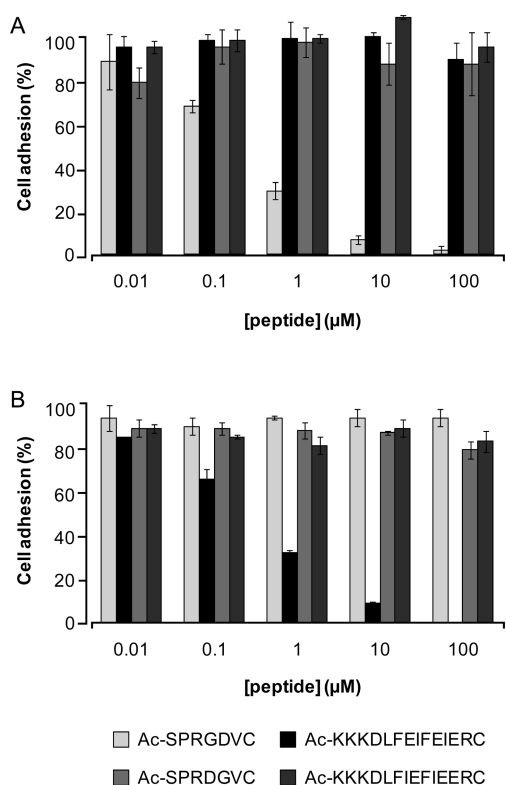


Figure 6. Inhibition of H4 cell adhesion to monolayers presenting SPRGDV (A) and KKKDLFEIFEIER (B). Cells were treated with soluble peptides at concentrations ranging from 0.01 to 100 μM and then allowed to adhere to model substrates. Scrambled soluble peptides did not inhibit cell adhesion. Cell adhesion was quantized as normalized units relative to adhesion in the absence of soluble inhibitors. Error bars are the standard error of three experiments.

including the use of optical and fluorescence microscopies. Significantly, these benefits make monolayers an effective approach for studies of ligand–receptor interactions in cell adhesion, and this work represents an early example of a study directed toward a current problem. We also note the recent work by Kiessling and co-workers, who used a similar strategy to find novel peptides that bound to receptors in pluripotent cells.¹⁸ Further, the compatibility of SAMDI mass spectrometry with the surfaces allows a straightforward and direct means to check the integrity of the substrate, including confirmation that the immobilization reactions have proceeded completely.

Multiple Ligands in ECM Proteins. The monolayers have proven particularly significant in studies of ECM proteins that present multiple ligands to a cell. Most ECM proteins present different ligands that each have a distinct specificity for binding to a receptor, and studies that aim to understand the role played by each ligand frequently give inconsistent results. The roles of the RGD and the PHSRN peptides in fibronectin, for example, are still debated despite extensive study.^{13,19,20} The monolayers offer a straightforward strategy to evaluate the activities of each ligand on adhesion—or a combination of both where synergistic effects operate—and to use inhibition experiments to determine whether the ligands bind overlapping or distinct sites on the receptor. These experiments were important to the work in this paper that has identified the FEI peptide in nephronectin as a RGD-independent ligand for the $\alpha 8\beta 1$ integrin. A similar approach was important to finding that the $\alpha \text{IIb}\beta 3$ integrin has

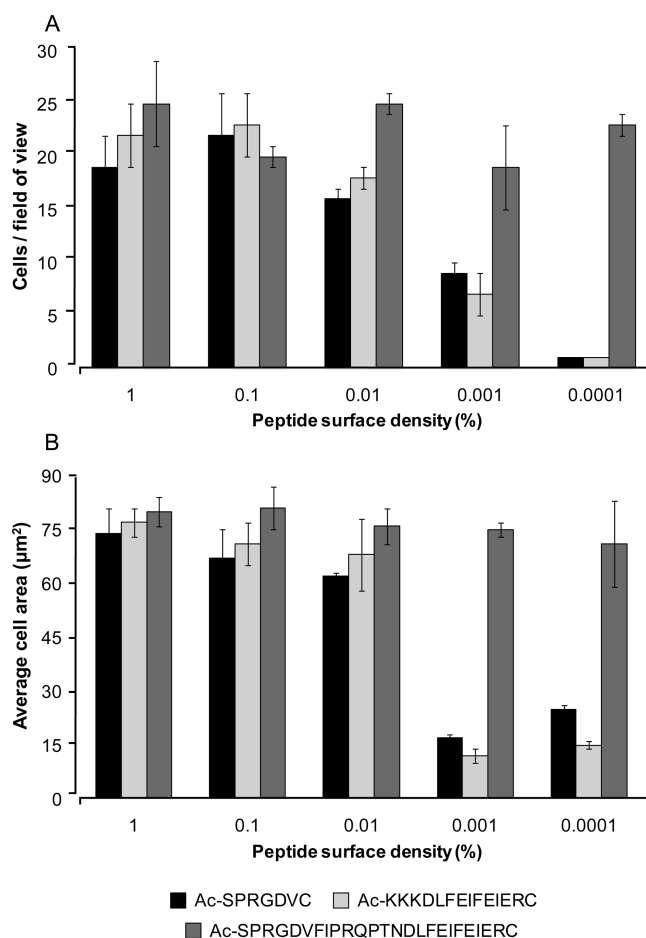


Figure 7. H4 cell adhesion and spreading on model substrates presenting peptide ligands at a range of densities. H4 cells were allowed to adhere (A) and spread (B) on monolayers presenting Ac-SPRGDVC, Ac-KKKDLFEIFEIERC, or Ac-SPRGDVFIPRQPTNDLFEIFEIERC at surface densities that ranged from 1% to 0.0001%. Cell adhesion was quantitated as cells per field of view, while cell spreading was quantitated by measuring the average cell area per surface. Error bars are the standard error of three experiments.

a relaxed specificity that allows it to bind the AGD segment in fibrinogen.¹⁵

In summary, we have demonstrated that the FEI motif in nephronectin can mediate cell adhesion independently of the RGD site. This ligand has specificity for the $\alpha 8\beta 1$ integrin and has a strict requirement for the glutamate residue but tolerates other aromatic residues in the first position and hydrophobic residues in the third position. Nephronectin has been implicated in a variety of biological processes, including kidney morphogenesis,^{6,7} osteogenesis,²¹ and tumor progression²² and has been found in lung and muscle tissue.¹⁷ The present work clarifies the roles of the two adhesive motifs in this protein and also provides a ligand that may be useful for selectively inhibiting or targeting the $\alpha 8\beta 1$ integrin.

METHODS

Antibodies and Reagents. All reagents were used as received. All amino acids and peptide synthesis reagents were purchased from Anaspec with the exception of resin lanterns, obtained from SynPhase. Anti-integrin antibodies F-19 (anti- $\alpha 8$) and M-106 (anti- $\beta 1$) were

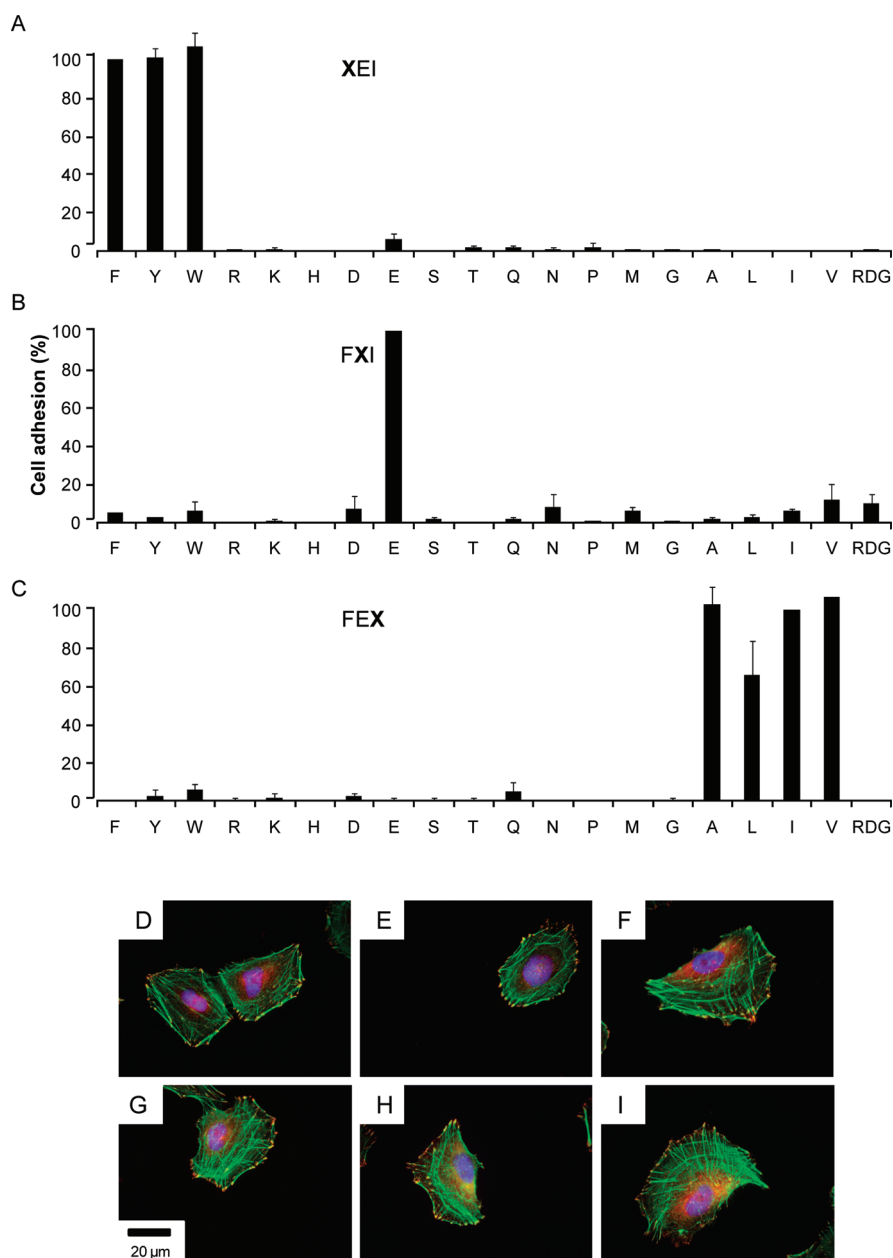


Figure 8. Structure–activity relationship for the FEI ligand in mediating cell adhesion. Arrays were employed to study H4 cell adhesion to the families of peptides GXEIGC (A), GFXIGC (B), and GFEXGC (C), where X is each amino acid except for cysteine. Cell adhesion was quantitated and is reported relative to adhesion to GFEIGC. Error bars are the standard error of three experiments. Immunostaining of adherent cells for those peptides that mediated adhesion (D–I): GFEAGC (D), GFELGC (E), GFEVGC (F), GFEIGC (G), GYEIGC (H), and GWEIGC (I). Focal adhesions were visualized with an antipaxillin antibody (red), actin stress fibers were visualized with AF 488 phalloidin (green), and nuclei were visualized with DAPI (blue). The scale bar in panel G applies to all panels.

purchased from Santa Cruz Biotechnology. MAB1956 (anti- $\alpha 5$) was obtained from Millipore. Monoclonal antipaxillin antibody, clone 5H11, was obtained from Millipore. Texas Red goat antimouse IgG and AF 488 phalloidin were obtained from Invitrogen. 4',6-Diamidino-2-phenylindole (DAPI) was obtained from Molecular Probes. Recombinant mouse nephronectin was obtained from R&D Systems. H4 cells were obtained from the American Tissue Culture Collection (ATCC). All cell culture media and reagents were obtained from Gibco. Formaldehyde was obtained from Ted Paella. All other reagents were purchased from Sigma-Aldrich.

Peptide Synthesis. All Cys-terminated peptides with the exception of peptides used for the cell adhesion array were synthesized manually following standard 9-fluorenylmethoxycarbonyl (Fmoc)

peptide synthesis protocols using Fmoc-Rink amide MBHA resin. All peptides were purified by reverse phase HPLC using a C18 column (Waters) and characterized with matrix-assisted laser desorption/ionization time of flight mass spectrometry (MALDI-TOF MS). Parallel synthesis of Ac-KKGFEXGC, Ac-KKGFYIGC, and Ac-KKGFYIGC peptide libraries where X were all amino acids except Cys was performed in 96-well filter plates with Fmoc-Rink amide MBHA resin lanterns (SynPhase) by using 15 equiv of benzotriazol-1-yl-oxytripyrrolidinophosphonium hexafluorophosphate (PyBOP)/N-methylmorpholine (NMM). Briefly, lanterns were placed in each well and deprotected with 20% piperidine in DMF (2×15 min). Fmoc amino acids were coupled in the presence of PyBOP and

NMM for 30 min. Each step was repeated twice to ensure coupling completion. After reaction, the lanterns were washed twice with DMF, and the coupling and deprotection steps were repeated until the desired sequences were obtained. During synthesis, all solutions were drained from the filter plate using a vacuum manifold. After the final Fmoc deprotection, the peptides were acetylated with 20% acetic anhydride in DMF, washed, and dried under nitrogen overnight. The lanterns were then placed in 96-well plates, and the peptides were cleaved from the lanterns using a cleavage solution of TFA/water/TIS 95:2.5:2.5, (v/v/v) for 2 h. The cleavage solution was dried under nitrogen, and the peptides were retrieved by adding DIUF water and lyophilizing.

Preparation of Monolayers. Glass coverslips were sonicated for 30 min in deionized ultrafiltered (DIUF) water followed by 30 min in ethanol and then dried under a stream of nitrogen. Titanium (4 nm) and then gold (29 nm) were evaporated onto the coverslips using an electron beam evaporator (Boc Edwards) at a rate of 0.05–0.10 nm/s and at a pressure of 1 μ Torr. The gold-coated coverslips were immersed in an ethanolic solution of both maleimide-terminated disulfide (2%) and tri(ethylene glycol)-terminated disulfide (98%) and incubated overnight at RT. For substrates used to adsorb protein, the gold-coated coverslips were immersed in an ethanolic solution of octadecanethiol. The total disulfide concentration for all types of substrates was 1 mM. The substrates were washed with DIUF water and ethanol and then dried under a stream of nitrogen.

Cell Adhesion Assays. Cysteine-terminated peptides were immobilized onto 1% maleimide-presenting SAMs by immersing the monolayers in a solution of peptide (1 mM in TRIS buffer, pH = 7.5) and incubated at 37 °C for 1 h. For substrates with adsorbed nephrolectin, octadecanethiolate monolayers were immersed in a buffered solution of recombinant protein (25 μ g/mL) and incubated at 37 °C for 1.5 h. All substrates were rinsed with DIUF water and dried under a stream of nitrogen prior to use. H4 cells were detached from culture plates with 1 mM EGTA/2 mM EDTA in PBS, rinsed with Dulbecco's Modified Eagle's medium (DMEM) (10% FBS, 4 mM L-glutamine, 25 mM D-glucose, 1X penicillin/streptomycin), centrifuged, and resuspended in the serum-free medium at a density of 60,000/mL. Cells were added to substrates in 24-well culture plates and incubated at 37 °C and 5% CO₂ for 30 min, after which media was changed to serum-containing DMEM for 1 h and incubated under the same conditions. Adherent cells were then treated with 4 μ M cytochalasin D for 1 h and allowed to recuperate from the treatment in serum-containing DMEM for an additional 1 h at 37 °C and 5% CO₂. Upon completion of the incubation period, substrates were washed gently with PBS and used for immunostaining.

Immunostaining. Adherent H4 cells were fixed and permeabilized with 4% formaldehyde and 0.5% Triton-X for 30 min. Fixed and permeabilized cells were blocked in the presence of blocking buffer (1% BSA, 5% goat serum, and 0.1% Triton-X) for 30 min. Substrates were then incubated with a 1:1000 dilution of monoclonal antipaxillin IgG (Sigma) for 30 min, followed by incubation with 1:400 dilution of phalloidin-AF488 and TR goat antimouse IgG and 1:5000 DAPI for 30 min. After extensive washing with blocking buffer, the substrates were mounted with Aqua Poly/Mount (PolySciences Inc.). Fluorescent images of cells on substrates were acquired with a 100 X objective of a Zeiss Axiovert 200 inverted microscope.

Antibody-Inhibited Adhesion. Suspensions of H4 cells (60,000/mL) were incubated with antibodies (1:500 dilution) for 10 min prior to addition to monolayer substrates. Cells were incubated in serum-free DMEM for 30 min at 37 °C and 5% CO₂, after which media was changed to serum-containing DMEM for 1 h and incubated under the same conditions. After incubation, the substrates were washed gently with warm PBS and adherent cells were immediately fixed and permeabilized with 4% formaldehyde and 0.5% Triton-X for 30 min. Fixed and permeabilized cells were stained with DAPI (1:5000) for

30 min and mounted with Aqua Poly/Mount (PolySciences Inc.). Fluorescent images of nuclei were acquired with a 20 X objective with a Zeiss Axiovert 200 inverted microscope. The number of adherent cells per field of view was counted using Image J. Cells were counted in at least five fields for each substrate, and each experiment was repeated 3 times. The degree of inhibition is reported as a percentage of cells that adhere relative to control experiments in the absence of soluble inhibitor. Standard error was used for error bars.

Cell Adhesion Assay to Truncated Peptides. H4 cells were added to monolayers presenting truncated peptides in serum-free DMEM for 30 min at 37 °C and 5% CO₂, after which media was changed to serum-containing DMEM for 1 h and incubated under the same conditions. After incubation, the substrates were washed gently with warm PBS and adherent cells were immediately fixed and permeabilized with 4% formaldehyde and 0.5% Triton-X for 30 min. Fixed and permeabilized cells were stained with DAPI (1:5000) for 30 min, and mounted with Aqua Poly/Mount (PolySciences Inc.). Fluorescent images of nuclei on substrates were acquired with a 20 X objective with a Zeiss Axiovert 200 inverted microscope. The number of adherent cells per field of view was counted using Image J. Cells were counted in at least five fields for each substrate, and each experiment was repeated 3 times. Cell adhesion is reported as a percentage of cells that adhere relative to control adhesion experiments to full-length peptides. Standard error was used for error bars.

Cell Adhesion Inhibition Assay. Suspensions of H4 cells (60,000/mL) were incubated with soluble inhibitors (Ac-SPRGDV, Ac-SPRDGV, Ac-KKKDLFEIFEIER, Ac-KKKDLFIEFIEER) for 10 min prior to their application to the monolayer substrates. Cells were incubated in serum-free DMEM for 30 min at 37 °C and 5% CO₂, after which media was changed to serum-containing DMEM for 1 h and incubated under the same conditions. After incubation, the substrates were washed gently with warm PBS, and adherent cells were immediately fixed and permeabilized with 4% formaldehyde and 0.5% Triton-X for 30 min. Fixed and permeabilized cells were stained with DAPI (1:5000) for 30 min and mounted with Aqua Poly/Mount (PolySciences Inc.). Fluorescent images of nuclei on substrates were acquired with a 20 X objective on a Zeiss Axiovert 200 inverted microscope. The number of adherent cells per field of view was counted using Image J. Cells were counted in at least five fields for each substrate, and each experiment was repeated 3 times. The degree of inhibition is reported as a percentage of cells that adhere relative to control experiments in the absence of soluble inhibitor. Standard error was used for error bars.

Cell Adhesion to Different Ligand Densities. H4 cells were added to monolayers presenting Ac-SPRGDVC, Ac-KKKDLFEIFEIER, or Ac-SPRGDVFIPRQPTNDLFEIFEIER at densities ranging from 1% to 0.0001% in serum-free DMEM supplemented with anti- α 5 antibody (1:500 dilution) for 30 min at 37 °C and 5% CO₂, after which media was changed to serum-containing DMEM supplemented with anti- α 5 antibody (1:500 dilution) for 1 h and incubated under the same conditions. After incubation, the substrates were washed gently with warm PBS, and adherent cells were immediately fixed and permeabilized with 4% formaldehyde and 0.5% Triton-X for 30 min. Fixed and permeabilized cells were stained with DAPI (1:5000) and phalloidin-AF488 (1:400) for 30 min and mounted with Aqua Poly/Mount (PolySciences Inc.). Fluorescent images of nuclei and actin cytoskeletons were acquired with a 20 X objective on a Zeiss Axiovert 200 inverted microscope. The number of adherent cells per field of view was counted using Image J. Cells were counted in at least five fields for each substrate, and each experiment was repeated 3 times. Standard error was used for error bars. Cell area for each field was obtained by thresholding the actin images using Image J to calculate the cell's area, obtaining an average cell area per field of view. Cells were analyzed in at least five fields for each substrate,

and each experiment was repeated 3 times. Standard error was used for error bars.

Cell Adhesion Assay to Peptide Arrays. Glass coverslips were patterned with gold circles as described.²³ Glass areas were passivated by reacting with undecyltrichlorosilane (70 mM in toluene) for 10 min at RT. After washing the substrate with toluene and ethanol and drying under a stream of nitrogen, peptides were immobilized on the circles as described previously. After washing, the arrays were immersed in a solution of BSA (25 $\mu\text{g}/\text{mL}$ in EXPLAIN BUFFER) and incubated at 37 °C for 1.5 h. H4 cells were added to peptide arrays presenting Ac-KKGFEXGC, Ac-KKGFIXGC, and Ac-KKGEIXGC peptide libraries, where X were all amino acids except Cys, in serum-free DMEM for 30 min at 37 °C and 5% CO₂, after which media was changed to serum-containing DMEM for 1 h and incubated under the same conditions. After incubation, the substrates were washed gently with warm PBS, and adherent cells were immediately fixed and permeabilized with 4% formaldehyde and 0.5% Triton-X for 30 min. Fixed and permeabilized cells were stained with DAPI (1:5000) for 30 min and mounted with Aqua Poly/Mount (PolySciences Inc.). Fluorescent images of cells' nuclei on substrates were acquired with a 20 X objective of a Zeiss Axiovert 200 inverted microscope. The number of adherent cells per field of view was counted using Image J. Cells were counted in at least five fields for each substrate, and each experiment was repeated 3 times. Cell adhesion is reported as a percentage of cells that adhere relative to control adhesion experiments to Ac-KKGFEXGC. Standard error was used for error bars. Adherent cells were also immunostained as described previously.

■ ASSOCIATED CONTENT

S Supporting Information. This material is available free of charge via the Internet at <http://pubs.acs.org>.

■ AUTHOR INFORMATION

Corresponding Author

*E-mail: mmrksich@uchicago.edu.

■ ACKNOWLEDGMENT

This work was supported by the National Institutes of Health (US4 CA151880).

■ REFERENCES

- (1) Gullberg, D. (2007) Neuronal Pathways Leading to the Kidney. *Matrix Biol.* 26, 407–408.
- (2) Humphries, J. D., Byron, A., and Humphries, M. J. (2006) Integrin Ligands at a Glance. *J. Cell Sci.* 119, 3901–3903.
- (3) Müller, U., Wang, D., Denda, S., Meneses, J. J., Pedersen, R. A., and Reichardt, L. F. (1997) Integrin $\alpha 8\beta 1$ Is Critically Important for Epithelial-Mesenchymal Interactions during Kidney Morphogenesis. *Cell* 88, 603–613.
- (4) Denda, S., Reichardt, L. F., and Müller, U. (1998) Identification of Osteopontin as a Novel Ligand for the Integrin $\alpha 8\beta 1$ and Potential Roles for this Integrin-Ligand Interaction in Kidney Morphogenesis. *Mol. Biol. Cell* 9, 1425–1435.
- (5) Liaw, L., Birk, D. E., Ballas, C. B., Whitsitt, J. S., Davidson, J. M., and Hogan, B. L. (1998) Altered Wound Healing in Mice Lacking a Functional Osteopontin Gene. *J. Clin. Invest* 101, 1468–1478.
- (6) Brandenberger, R., Schmidt, A., Linton, J., Wang, D., Backus, C., Denda, S., Müller, U., and Reichardt, L. F. (2001) Identification and Characterization of a Novel Extracellular Matrix Protein Nephronectin that is Associated with Integrin $\alpha 8\beta 1$ in the Embryonic Kidney. *J. Cell Biol.* 154, 447–458.
- (7) Linton, J. M., Martin, G. R., and Reichardt, L. F. (2007) The ECM Protein Nephronectin Promotes Kidney Development via Integrin $\alpha 8\beta 1$ -Mediated Stimulation of *Gdnf* Expression. *Development* 134, 2501–2509.
- (8) Morimura, N., Tezuka, Y., Watanabe, N., Yasuda, M., Miyatani, S., Hozumi, N., and Tezuka, K. (2001) Molecular Cloning of POEM: a Novel Adhesion Molecule that Interacts with $\alpha 8\beta 1$ Integrin. *J. Biol. Chem.* 276, 42172–42181.
- (9) Sato, Y., Uemura, T., Morimitsu, K., Sat-Nishiuchi, R., Manabe, R., Takagi, J., Yamada, M., and Sekiguchi, K. (2009) Molecular Basis of the Recognition of Nephronectin by Integrin $\alpha 8\beta 1$. *J. Biol. Chem.* 284, 14524–14536.
- (10) Mrksich, M. (2009) Using Self-Assembled Monolayers to Model the Extracellular Matrix. *Acta Biomater.* 5, 832–841.
- (11) Ramsden, J. J., Roush, D. J., Gill, D. S., Kurrat, R., and Willson, R. C. (1995) Protein Adsorption Kinetics Drastically Altered by Repositioning a Single Charge. *J. Am. Chem. Soc.* 117, 8511–8516.
- (12) Basbaum, C. B., and Werb, Z. (1996) Focalized Proteolysis: Spatial and Temporal Regulation of Extracellular Matrix Degradation at the Cell Surface. *Curr. Opin. Cell Biol.* 8, 731–738.
- (13) Feng, Y., and Mrksich, M. (2004) The Synergy Peptide PHSRN and the Adhesion Peptide RGD Mediate Cell Adhesion through a Common Mechanism. *Biochemistry* 43, 15811–15821.
- (14) Eisenberg, J. L., Piper, J. L., and Mrksich, M. (2009) Using Self-Assembled Monolayers to Model Cell Adhesion to the 9th and 10th Type III Domains of Fibronectin. *Langmuir* 25, 13942–13951.
- (15) Sánchez-Cortés, J., and Mrksich, M. (2009) The Platelet Integrin $\alpha \text{IIb}\beta 3$ Binds to the RGD and AGD Motifs in Fibrinogen. *Chem. Biol.* 16, 990–1000.
- (16) Kato, M., and Mrksich, M. (2004) Using Model Substrates To Study the Dependence of Focal Adhesion Formation on the Affinity of Integrin-Ligand Complexes. *Biochemistry* 43, 2699–2707.
- (17) Schnapp, L. M., Breuss, J. M., Ramos, D. M., Sheppard, D., and Pytela, R. (1995) Sequence and Tissue Distribution of the Human Integrin $\alpha 8$ Subunit: A $\beta 1$ -Associated α Subunit Expressed in Smooth Muscle Cells. *J. Cell Sci.* 108, 537–544.
- (18) Derda, R., Musah, S., Orner, B. P., Klim, J. R., Li, L., and Kiessling, L. L. (2010) High-Throughput Discovery of Synthetic Surfaces That Support Proliferation of Pluripotent Cells. *J. Am. Chem. Soc.* 132, 1289–1295.
- (19) Grant, R. P., Spitzfaden, C., Altmann, H., and Campbell, I. D. (1997) Structural Requirements for Biological Activity of the Ninth and Tenth FIII Domains of Human Fibronectin. *J. Biol. Chem.* 272, 6159–6166.
- (20) Bowditch, R. D., Hariharan, M., Tominna, E. F., Smith, J. W., Yamada, K. M., Getzoff, E. D., and Ginsberg, M. H. (1994) Identification of a Novel Integrin Binding Site in Fibronectin. *J. Biol. Chem.* 269, 10856–10863.
- (21) Kahai, S., Lee, S.-C., Seth, A., and Yang, B. B. (2010) Nephronectin Promotes Osteoblast Differentiation via the Epidermal Growth Factor-Like Repeats. *FEBS Lett.* 584, 233–238.
- (22) Kuphal, S., Wallner, S., and Bosserhoff, A. K. (2008) Loss of Nephronectin Promotes Tumor Progression in Malignant Melanoma. *Cancer Sci.* 99, 229–233.
- (23) Min, D. H., Yeo, W. S., and Mrksich, M. (2004) A Method for Connecting Solution-Phase Enzyme Activity Assays with Immobilized Format Analysis by Mass Spectrometry. *Anal. Chem.* 76, 3923–3929.